Author/s:
Keating, MF;Yang, C;Liu, Y;Gould, EA;Hallam, MT;Henstridge, DC;Mellett, NA;Meikle, PJ;Watt, KI;Gregorevic, P;Calkin, AC;Drew, BG

Title:
Hepatic retinol dehydrogenase 11 dampens stress associated with the maintenance of cellular cholesterol levels

Date:
2024-12-01

Citation:
Keating, M. F., Yang, C., Liu, Y., Gould, E. A., Hallam, M. T., Henstridge, D. C., Mellett, N. A., Meikle, P. J., Watt, K. I., Gregorevic, P., Calkin, A. C. & Drew, B. G. (2024). Hepatic retinol dehydrogenase 11 dampens stress associated with the maintenance of cellular cholesterol levels. Molecular Metabolism, 90, https://doi.org/10.1016/j.molmet.2024.102041.

Persistent Link:
https://hdl.handle.net/11343/358939

Original Article

MOLECULAR METABOLISM

Hepatic retinol dehydrogenase 11 dampens stress associated with the maintenance of cellular cholesterol levels

Michael F. Keating[1,2], Christine Yang[1], Yingying Liu[1], Eleanor AM. Gould[1], Mitchell T. Hallam[1,4], Darren C. Henstridge[3], Natalie A. Mellett[1], Peter J. Meikle[1,2,4,5], Kevin I. Watt[6], Paul Gregorevic[7,8,9], Anna C. Calkin[1,2,4,10], Brian G. Drew[1,2,4,5,*,10]

ABSTRACT

Objective: Dysregulation of hepatic cholesterol metabolism can contribute to elevated circulating cholesterol levels, which is a significant risk factor for cardiovascular disease. Cholesterol homeostasis in mammalian cells is tightly regulated by an integrated network of transcriptional and post-transcriptional signalling pathways. Whilst prior studies have identified many of the central regulators of these pathways, the extended supporting networks remain to be fully elucidated.

Methods: Here, we leveraged an integrated discovery platform, combining multi-omics data from 107 strains of mice to investigate these supporting networks. We identified retinol dehydrogenase 11 (RDH11; also known as SCALD) as a novel protein associated with cholesterol metabolism. Prior studies have suggested that RDH11 may be regulated by alterations in cellular cholesterol status, but its specific roles in this pathway are mostly unknown.

Results: Here, we show that mice fed a Western diet (high fat, high cholesterol) exhibited a significant reduction in hepatic *Rdh11* mRNA expression. Conversely, mice treated with a statin (3-hydroxy-3-methyl-glutaryl-coenzyme A reductase (HMGCR) inhibitor) exhibited a 2-fold increase in hepatic *Rdh11* mRNA expression. Studies in human and mouse hepatocytes demonstrated that *RDH11* expression was regulated by altered cellular cholesterol conditions in a manner consistent with SREBP2 target genes *HMGCR* and *LDLR*. Modulation of RDH11 *in vitro* and *in vivo* demonstrated modulation of pathways associated with cholesterol metabolism, inflammation and cellular stress. Finally, RDH11 silencing in mouse liver was associated with a reduction in hepatic cardiolipin abundance and a concomitant reduction in the abundance of proteins of the mitochondrial electron transport chain.

Conclusion: Taken together, these findings suggest that RDH11 likely plays a role in protecting cells against the cellular toxicity that can arise as a by-product of endogenous cellular cholesterol synthesis.

Keywords Cholesterol metabolism; Lipid metabolism; Oxidative stress; Inflammation; Lipidomics; Mitochondrial biology; Systems genetics

1. INTRODUCTION

Cholesterol homeostasis is critical for the normal functioning of mammalian cells. Specifically, cholesterols contribute to the maintenance of plasma membrane structure, act as signalling molecules and as precursors for numerous metabolites including steroid hormones [1]. In mammals, the primary site of endogenous cholesterol synthesis is the liver. This process is principally driven by two transcription factors, sterol response element binding protein (SREBP) 2 and liver X receptor (LXR), which act in an opposing manner to promote cholesterol synthesis and uptake, and cholesterol efflux, respectively [2,3]. Dysregulation of hepatic cholesterol homeostasis can precipitate elevated serum cholesterol levels, known as hypercholesterolemia, which is a significant risk factor for cardiovascular diseases (CVD) [4]. The strong association between hypercholesterolemia and CVD has fuelled interest in understanding the regulatory pathways that contribute to cholesterol homeostasis, with the hope of identifying novel targets for therapeutic intervention. One approach to identify

[1]Baker Heart and Diabetes Institute, Melbourne, Victoria, Australia [2]Baker Department of Cardiometabolic Disease, University of Melbourne, Melbourne, Victoria, Australia [3]School of Health Sciences, College of Health and Medicine, University of Tasmania, Launceston, Tasmania, Australia [4]Central Clinical School, Department of Medicine, Monash University, Melbourne, Victoria, Australia [5]Baker Department of Cardiovascular Research Translation and Implementation, La Trobe University, Bundoora, Victoria, Australia [6]Novo Nordisk Foundation Centre for Stem Cell Medicine (reNEW), Murdoch Children's Research Institute, Melbourne, Victoria, Australia [7]Centre for Muscle Research, Department of Anatomy & Physiology, University of Melbourne, Parkville, Victoria 3010, Australia [8]Department of Biochemistry and Molecular Biology, Monash University, VIC 3800, Australia [9]Department of Neurology, University of Washington School of Medicine, Seattle, WA 98195, USA

[10] Anna C. Calkin and Brian G. Drew contributed equally.

*Corresponding author. Baker Heart and Diabetes Institute, Melbourne, Victoria, Australia. E-mail: brian.drew@baker.edu.au (B.G. Drew).

Received July 9, 2024 • Revision received September 24, 2024 • Accepted September 25, 2024 • Available online 2 October 2024

https://doi.org/10.1016/j.molmet.2024.102041

novel drivers of complex traits such as hypercholesterolemia is to utilise genetic reference panels (GRPs). GRPs exploit model organisms such as mice, fruit flies or roundworms, and investigate how genetic variance influences phenotypic outcomes, a process analogous to human genome wide association studies. GRPs have been utilised to identify numerous novel loci implicated in conditions associated with lipid dysregulation, including obesity [5]. Indeed, our group has previously demonstrated the utility of a mouse GRP known as the Hybrid Mouse Diversity Panel (HMDP) to map genes important in the regulation of lipid metabolism [6]. Specifically, by integrating plasma and liver proteomic and lipidomic analyses, we could successfully identify both known and novel regulators of hepatic lipid metabolism [6]. Here, we utilise these previously generated datasets to identify novel proteins associated with cholesterol metabolism, including retinol dehydrogenase 11 (RDH11).

RDH11 is a microsomal short chain dehydrogenase/reductase that has oxido-reductive affinity for all *trans* and *cis* retinols, retinals and aldehyde species [7]. Initial RDH11 characterisation studies demonstrated that it was highly expressed in the human prostate epithelium [8]. These studies also identified RDH11 to be responsive to synthetic androgens. Further studies have suggested that mouse RDH11 could react with toxic C_2—C_{12} fatty aldehyde species, including 4-hydroxy-2-nonenal, to produce non-toxic fatty alcohol species [9]. More recently, studies in retinal pigment epithelial cells have implicated RDH11 in maintaining healthy visual function, acting to replenish all-*trans* and 11-*cis* aldehyde isomers [10]. Brown and Goldstein have previously suggested that RDH11 expression is induced by SREBPs [9]. Similarly, expression array analysis utilising human immortalised lymphoblastoid cell lines exposed to simvastatin demonstrated that RDH11 correlated with 3-hydroxy-3-methyl-glutaryl-coenzyme A reductase (HMGCR) [11], the rate-limiting enzyme in the cholesterol biosynthesis pathway. Moreover, analysis of multi-species transcriptomic data by Gene-Module Association Determination, and Module-Module Association Determination, suggested that the function of RDH11 may relate to cholesterol metabolism and be conserved across humans and rodents [12]. Very recently, RDH11 was further identified through a genetic screen of 35 strains of mice to be co-correlated with cholesterol biosynthetic genes [13], and subsequently suggested in that study to be involved in the modulation of endogenous cholesterol levels in cultured cells.

Here, we examined the role of RDH11 both *in vitro* and *in vivo* in the context of cholesterol metabolism, to build on its recognised functions as well as its potential roles in inflammatory and oxidative pathways.

2. RESULTS

2.1. Identification of RDH11 utilising the hybrid mouse diversity panel

To identify potential novel regulators of hepatic cholesterol metabolism we examined a multi-omics dataset derived from the hybrid mouse diversity panel (HMDP) [6]. Briefly, 107 strains of inbred mice from the HMDP ($n = 2$—3 mice per strain; 307 mice in total) were fed a chow diet for approximately 8 weeks. Mice were fasted overnight, then blood and tissue collected for proteomic and lipidomic phenotyping (Figure 1A). Specifically, liver proteomic analysis detected 8370 proteins, of which 4311 proteins were present across at least 50 strains. Lipidomic analysis of the liver and plasma quantified 313 and 307 lipid species, respectively. From these data we constructed protein—protein co-correlations across the HMDP using known regulators of cholesterol metabolism. This included NAD(P) Dependent Steroid Dehydrogenase-Like (NSDHL), Acyl-coenzyme A synthetase short-chain family member 2 (ACSS2), Farnesyl pyrophosphate synthase (FDPS), Cytochrome P450 Family 51 Subfamily A Member 1 (Cyp51a1), Transmembrane 7 Superfamily Member 2 (TM7SF2), Isopentenyl-Diphosphate Delta Isomerase 1 (IDI1) and 24-Dehydrocholesterol Reductase (DHCR24). This approach was performed on the premise that proteins with related functions are likely to be co-regulated, and thus high concordance in their correlation structure will provide an informative insight into proteins that participate in related pathways, and indeed, we showed this to be true for many pathways in our previous study [6]. This analysis identified both known and novel proteins that co-correlated with the aforementioned established regulators of cholesterol metabolism (Figure 1B—D; Supp Figure 1A-D). RDH11 was amongst the top 25 statistically significant proteins that correlated with all seven cholesterol biosynthetic proteins for which protein—protein correlation analyses were performed. We also performed protein-lipid correlation analyses utilising liver and plasma lipidomic analyses. Despite the co-correlation with known regulators of cholesterol metabolism, analyses revealed that RDH11 did not significantly correlate with hepatic or plasma total cholesterol ester (CE) or hepatic free cholesterol (COH) abundance across the HMDP (Supp Figure 1E-G; Supp Tables 2 and 3), however, there was a significant correlation with plasma COH levels ($p < 0.05$; Supp Figure 1H).

Next, we used RDH11 as a seed (hub) protein and performed a co-correlation analysis across the HMDP liver proteome (Figure 1E). The top statistically significant protein correlation with RDH11 was transmembrane 7 Superfamily Member 2 (TM7SF2), a core cholesterol biosynthesis enzyme (bicor 0.5455; $q = 4.7 \times 10^{-24}$). Moreover, of the top 50 statistically significant proteins that correlated with RDH11, 15 of which were linked to lipid metabolism, including both cholesterol synthesis and fatty acid metabolism. Moreover, pathway enrichment analysis of these correlated proteins identified processed linked to lipid metabolism as well as mitochondrial biology to be the most enriched (Figure 1F). Taken together, these data are suggestive of a role for RDH11 in the context of cholesterol metabolism, with the potential to impact on associated pathways including oxidative stress.

2.2. Endogenous *RDH11* gene expression is transcriptionally regulated by intracellular cholesterol status

Given this strong correlative evidence suggesting a role for RDH11 in cholesterol metabolism, we next sought to examine whether hepatic *Rdh11* mRNA expression in mice was modulated by an altered cholesterol environment. Indeed, we demonstrated this was the case. Specifically, mice fed a western diet (high fat, high cholesterol; WD) exhibited a significant reduction in hepatic *Rdh11* mRNA expression compared to mice fed a chow diet for 16 weeks ($p < 0.001$; Figure 2A). In contrast, mice fed a high fat diet (HFD), which lacks cholesterol, had no effect on hepatic *Rdh11* mRNA expression compared to chow fed mice, suggesting that RDH11 expression was responsive to the presence of cholesterol rather than excess dietary fat. Conversely, hepatic *Rdh11* mRNA expression was significantly increased in mice that received the 3-hydroxy-3-methyl-glutaryl-coenzyme A reductase (HMGCR) inhibitor, simvastatin, for 2 weeks, compared to those that received vehicle control ($p < 0.05$; Figure 2B). These findings highlight the reciprocal transcriptional regulation of RDH11 in response to an altered cholesterol environment.

To further explore the transcriptional regulation of *RDH11* in the setting of altered cholesterol metabolism, we utilised a human hepatoma cell line, Hep3B. These cells were exposed to altered sterol conditions that mimic a high or low cholesterol environment, for 24 h. To confirm that our cholesterol modulating agents were working as expected, we assessed the mRNA expression of three key genes integral to the

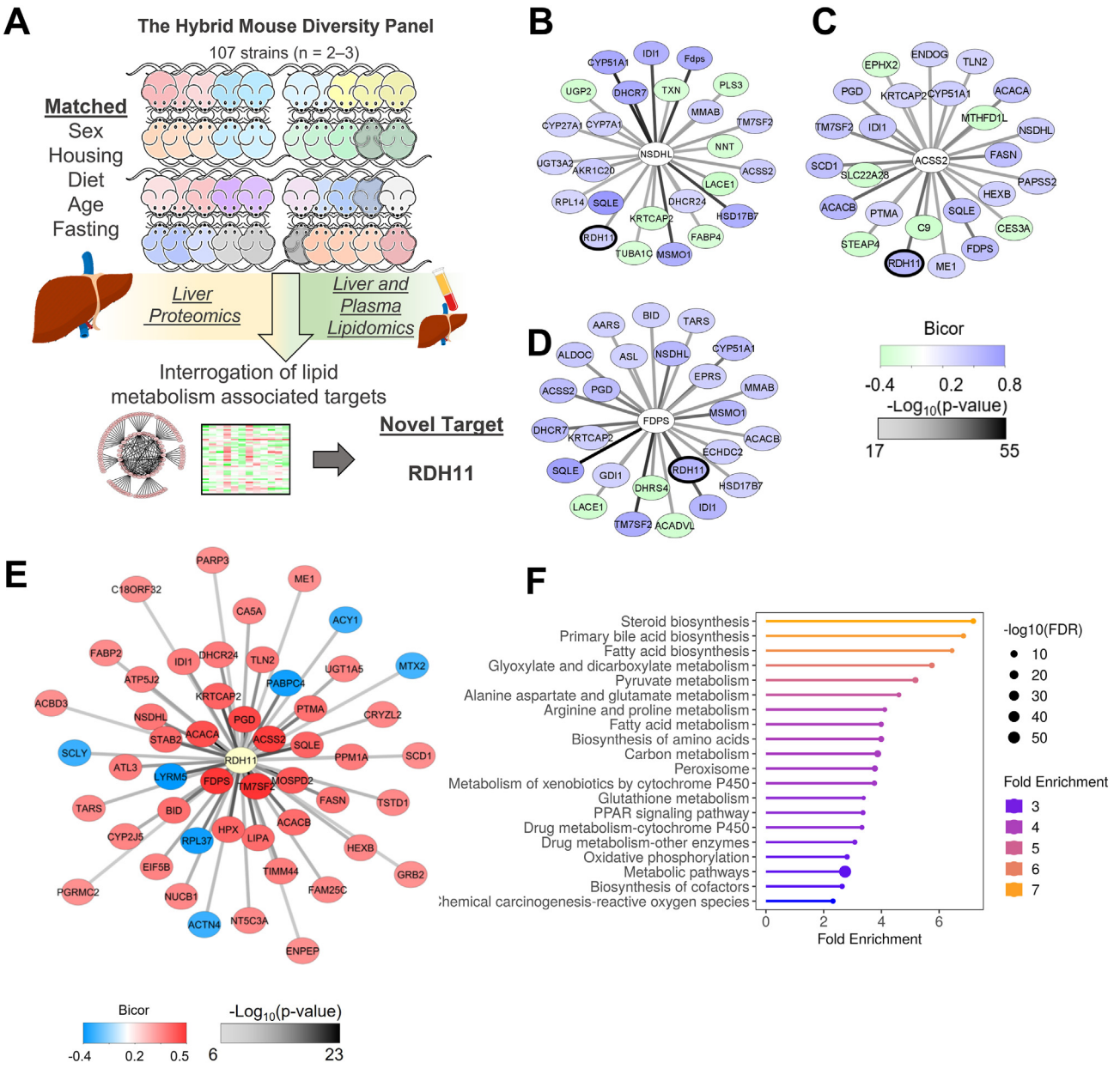

Figure 1: Co-correlation analysis of liver proteomics data from the hybrid mouse diversity panel (HMDP) identified retinol dehydrogenase 11 (RDH11) as a potential novel regulator of cholesterol metabolism (**A**) Schema of the Hybrid Mouse Diversity Panel (HMDP) discovery platform published in Parker et al. [6]; (**B**–**D**) Linear corrected hepatic protein co-correlation networks of top 25 proteins significantly associated with known regulators of cholesterol metabolism (white nodes; centre) including (**B**) NAD(P) dependent steroid dehydrogenase-like (NSDHL), (**C**) acyl-coA synthetase short-chain family member 2 (ACSS2) and (**D**) farnesyl diphosphate synthase (FDPS) across at least 50 strains of mice from the HMDP, with RDH11 highlighted in black oval; (**E**) Linear corrected hepatic protein co-correlation network of top 50 proteins significantly associated with RDH11 across at least 50 strains of mice from the HMDP. **B-E**, line width (black > grey) is indicative of statistical significance following Benjamini Hochberg correction; Colour of node indicates bicorrelation (bicor) direction and strength as indicated in key. (**F**) Pathway enrichment analysis of the 422 proteins significantly correlated with RDH11 across the HMDP following Benjamini Hochberg correction. (For interpretation of the references to color in this figure legend, the reader is referred to the Web version of this article).

regulation of cellular cholesterol; the low-density lipoprotein receptor (LDLR; uptake), HMGCR (synthesis) and ATP binding cassette A1 (ABCA1; efflux). In response to conditions mimicking a high cholesterol environment, including full serum (FS), and 25-hydroxycholesterol (25HC), *LDLR and HMGCR* mRNA expression were reduced compared to control (lipoprotein deficient serum alone, LPDS) but not with cholesterol loaded cyclodextrin (CD/Chol) treatment (Figure 2C). Whilst *ABCA1* expression was increased in response to 25HC, CD/Chol and in response to treatment with T0901317 (T0) compound, a synthetic LXR agonist which promotes ABCA1 expression (Figure 2C). In response to agents that mimic a low cholesterol environment (compactin/mevalonate, CPN/Mev and cyclodextrin, CD), an opposing effect was observed (Figure 2C). *RDH11* mRNA expression was altered by these cellular treatments in a manner consistent with *LDLR* and *HMGCR* (LPDS vs 25HC, $p < 0.05$; LPDS vs CPN/Mev, $p < 0.01$; LPDS vs CD $p < 0.05$; Figure 2D). These data demonstrate that *RDH11* expression in the liver is likely regulated by SREBP2, albeit to a lesser degree than LDLR and HMGCR under these conditions.

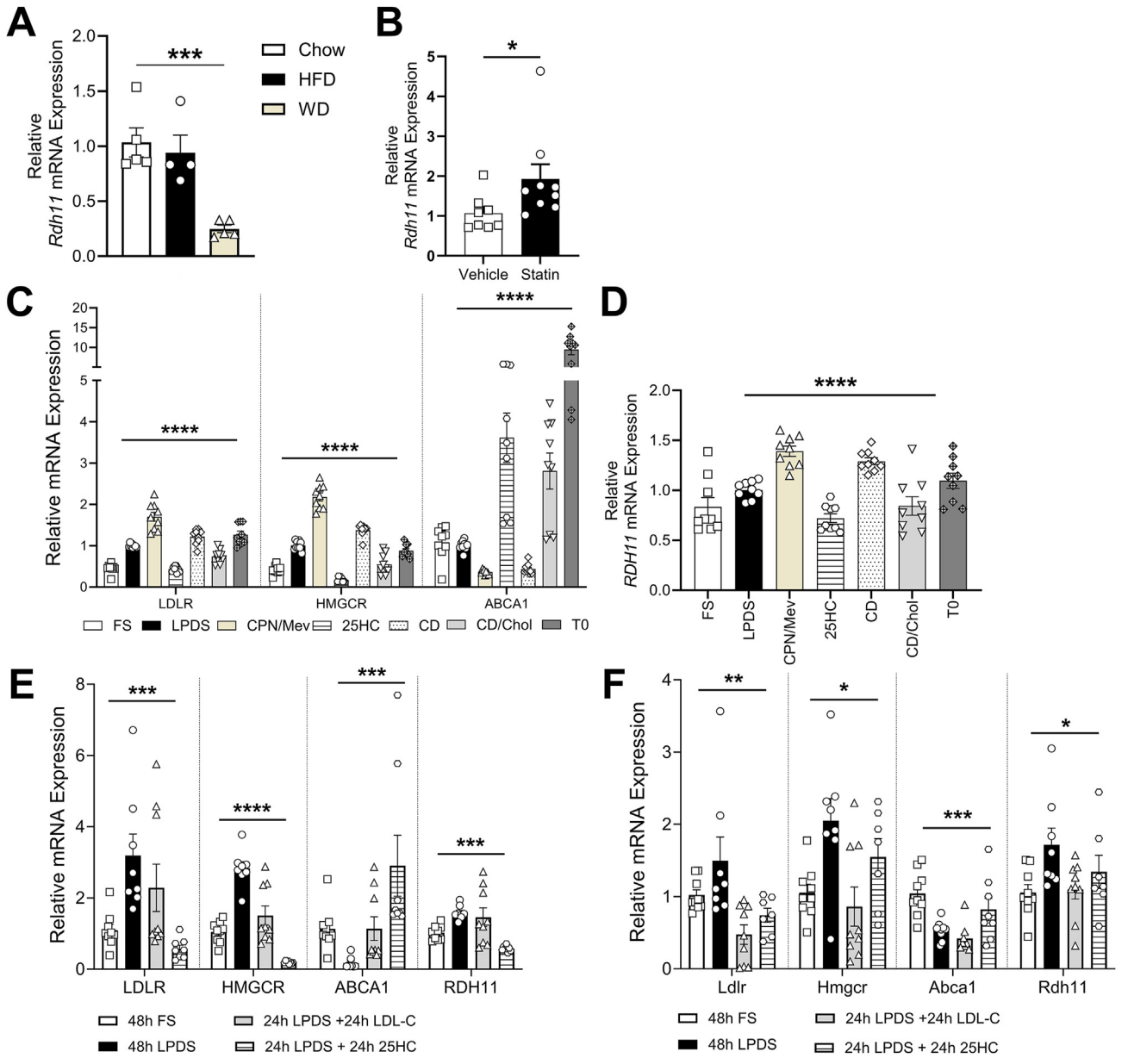

Figure 2: Retinol dehydrogenase 11 is transcriptionally responsive to altered cholesterol conditions Hepatic retinol dehydrogenase 11 (RDH11) mRNA expression in (**A**) mice fed a chow, high fat diet (HFD) or western diet (WD) for 16 weeks (n = 4–5/group) and (**B**) mice administered vehicle or simvastatin daily for 14 days (n = 8–9/group); (**C**) mRNA expression of low density lipoprotein receptor (LDLR), 3-hydroxy-3-methyl-glutaryl-coenzyme A reductase (HMGCR), ATP binding cassette transporter A1 (ABCA1) and (**D**) RDH11 in Hep3B cells treated with agents to induce high or low cholesterol conditions as indicated; mRNA expression in (**E**) Hep3B cells and (**F**) mouse primary hepatocytes exposed to cholesterol conditions as indicated; FS, full serum; LPDS, lipoprotein deficient serum; CPN/Mev compactin/mevalonate; 25HC, 25-hydroxycholesterol; CD, cyclodextrin; CD/Chol, cyclodextrin loaded cholesterol; T0, T0901317; LDL-C, low density lipoprotein cholesterol; Data presented as mean ± SEM; (**C**–**F**) n = 3 independent experiments, performed in triplicate. Data were analysed by Kruskal Wallis test (**A, C**–**F**), one-way ANOVA (**E, F**) or unpaired t-test (**B**); *p < 0.05, **p < 0.01 ***p < 0.001 and ****p < 0.0001.

To further confirm that the transcriptional regulation of *RDH11* was sensitive to cellular cholesterol status, we performed add-back experiments in Hep3B cells and mouse primary hepatocytes (Figure 2E, F). In human Hep3B cells, upon depletion of intracellular cholesterol levels for 48 h, mRNA expression of the SREBP2 target genes, *LDLR and HMGCR,* was increased compared to FS (*LDLR*, $p < 0.05$; *HMGCR* $p < 0.01$; Figure 2E). Conversely, *ABCA1* mRNA expression was significantly reduced ($p < 0.01$). When cells were depleted of cholesterol for 24 h, followed by LDL cholesterol (LDL-C) add-back for a further 24 h (total 48 h) to raise intracellular cholesterol levels, mRNA expression of SREBP2 genes reverted to levels observed with FS, with an even greater effect seen with 25HC add-back (*HMGCR,* $p < 0.05$). Like *LDLR* and *HMGCR*, *RDH11* mRNA expression was also increased in response to LPDS ($p < 0.05$), and was significantly reduced with supplementation of 25HC, compared to FS ($p < 0.05$).

To confirm that these observations were not cell line or species specific, we performed replicate studies in mouse primary hepatocytes. Whilst greater variability was observed in mouse hepatocytes, the data

mostly recapitulated that observed in human Hep3B cells, with the magnitude of response of *Rdh11* mRNA expression to altered cholesterol conditions similar to that seen with *Ldlr* and *Hmgcr* (Figure 2F). Together, these data confirm the responsiveness of *RDH11* mRNA expression to altered cholesterol levels *per se*, and further highlight the similarity in the transcriptional profile of RDH11 to other SREBP2 target genes in both mouse and human systems.

2.3. RDH11 modulates markers of cholesterol metabolism, inflammation and oxidative stress *in vitro*

Having observed that RDH11 mRNA expression is altered in relation to cholesterol exposure, we sought to determine whether RDH11 played a causal role in the regulation of cholesterol metabolism *in vitro*. Hep3B cells were transiently transfected with an empty vector (control) or plasmid containing the RDH11 cDNA for 24 h, then subjected to high or low cholesterol conditions for a further 24 h. We observed a significant ~2-fold increase in *RDH11* expression in control treated cells in response to a low cholesterol environment, consistent with findings shown above ($p < 0.01$; Figure 3A). Similarly, we confirmed protein overexpression using our RDH11 construct by western blotting (Supp Figure 2A). *RDH11* expression was also robustly increased in cells transfected with RDH11-plasmid, regardless of the cholesterol conditions ($p < 0.0001$; Figure 3A). We then assessed the effect of ectopic RDH11 expression on key markers of cholesterol regulation (Figure 3B). *LDLR* mRNA expression was elevated in response to low cholesterol conditions in control treated cells ($p < 0.0001$), and this effect was attenuated by

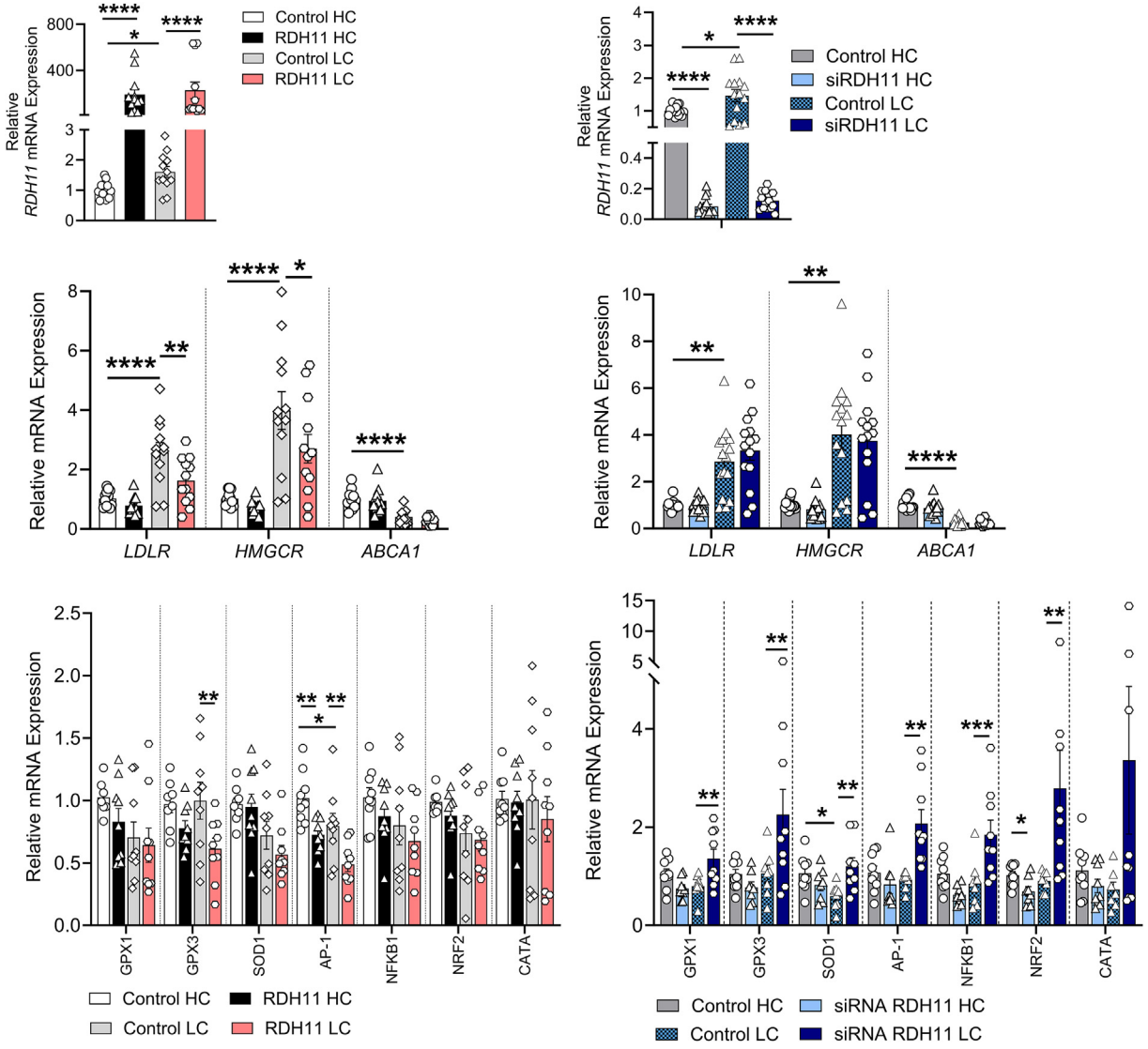

Figure 3: Retinol dehydrogenase 11 drives changes in genes linked to cholesterol metabolism, oxidative stress, and inflammation in Hep3B cells Relative mRNA expression of (**A, C**) RDH11 (**B, D**) genes linked to cholesterol metabolism and (**E, F**) genes linked to oxidative stress and inflammation in Hep3B cells transfected with (**A, B, E**) empty vector (control) or pcDNA:RDH11 for 24 h or (**C, D, F**) scramble siRNA (control) or siRNA RDH11 followed by exposure to a high cholesterol (HC; full serum) or low cholesterol (LC; LPDS+5 μM compactin + 50 μM mevalonate) environment for 24 h and expressed relative to the respective control HC; RDH11, retinol dehydrogenase 11; LDLR, low density lipoprotein receptor; HMGCR, 3-hydroxy-3-methyl-glutaryl-coenzyme A reductase; ABCA1, ATP binding cassette transporter A1; GPX, glutathione peroxidase; SOD1, superoxide dismutase 1; AP-1, activator protein 1, NFKB1, nuclear factor NF-kappa-B1; NRF2, nuclear factor erythroid 2-related factor 2; CATA, catalase; Data presented as mean ± SEM; n = 3–5 independent experiments, performed in triplicate. Data were analysed by Mann–Whitney test (**A, C**), Unpaired t-test (**C**) two-way ANOVA (**B, E, F**) or Kruskal–Wallis test (**D, F**) *$p < 0.05$, **$p < 0.01$ ***$p < 0.001$ and ****$p < 0.0001$.

increasing RDH11 expression in low cholesterol conditions ($p < 0.01$). Similarly, *HMGCR* mRNA expression was increased in the control cells in low compared to high cholesterol conditions ($p < 0.0001$), an effect that was also attenuated by increased RDH11 expression in low cholesterol conditions ($p < 0.05$). Lastly, *ABCA1* mRNA expression was markedly reduced in response to low cholesterol ($p < 0.0001$), however no effect of ectopic RDH11 was observed.

To assess whether physiological reduction of RDH11 would have reciprocal effects on SREBP2 target gene expression, cells were transfected with pooled control or RDH11 siRNAs (siRDH11) prior to exposure of cells to high or low cholesterol conditions for 24 h. *RDH11* mRNA expression was robustly downregulated ($p < 0.0001$) in the siRDH11 treated cells, and this was comparable regardless of the cholesterol conditions (Figure 3C). *LDLR* and *HMGCR* mRNA expression were increased ($p < 0.01$), and ABCA1 expression decreased ($p < 0.0001$), in response to a low cholesterol environment. RDH11 knockdown did not affect the expression of any of these genes in either high or low cholesterol conditions (Figure 3D). Collectively, these data indicate that in low cholesterol conditions where endogenous cholesterol synthesis is induced, increased expression of RDH11 drives a reduction in genes involved in the uptake and synthesis of cholesterol, a transcriptional response that is consistent with an attenuation of cholesterol accumulation.

The lack of effect of RDH11 knockdown on markers of cholesterol metabolism, prompted us to consider that, although RDH11 was transcriptionally regulated by cellular cholesterol abundance, its function may be related to other pathways associated with cholesterol biosynthesis such as oxidative stress and inflammation, rather than directly influencing cholesterol biosynthesis *per se*. This is consistent with the previously established role of RDH11 in the protection against oxidative stress associated with light exposure in the retina [14]. We therefore investigated the expression of genes associated with oxidative stress and inflammatory pathways in Hep3B cells following either RDH11 gain- or loss-of-function (Figure 3E, F). Overexpression of RDH11 was associated with a reduction in markers of oxidative stress and inflammation (Figure 3E). Specifically, in both high and low cholesterol conditions, expression of activator protein 1 (*AP-1*), a transcription factor involved in inflammation, cell signalling and apoptosis [15], was reduced by RDH11 overexpression ($p < 0.01$). Furthermore, ectopic expression of RDH11 attenuated expression of glutathione peroxidase (*GPX*) 3, which is implicated in the management of cellular organic hydroperoxide levels, in low cholesterol conditions only ($p < 0.01$) [16]. These data suggest that RDH11 can influence oxidative stress and inflammatory pathways regardless of cholesterol status, although the magnitude of effect was greater in a low cholesterol environment. RDH11 loss of function only significantly affected expression of NRF2 ($p < 0.05$) in a high cholesterol environment; however, in cells subjected to low cholesterol conditions, RDH11 silencing was associated with a significant increase in the expression of *GPX1* ($p < 0.01$), *GPX3* ($p < 0.01$) and superoxide dismutase 1 (*SOD1;* $p < 0.01$), *AP-1* ($p < 0.01$), nuclear factor kappa B subunit 1 (*NFκB1;* $p < 0.001$) and nuclear factor erythroid 2-related factor *2* (*NRF2*; $p < 0.01$) compared to control treated cells (Figure 3F). These data suggest that in the absence of RDH11, there is an upregulation of markers of inflammatory and oxidative pathways.

Finally, we considered whether RDH11 gain- or loss-of-function was affecting retinol metabolism, given its function as a retinol dehydrogenase. We observed no significant change in transcriptional markers of retinol metabolism including beta-carotene oxygenase 2 (*BCO2),* retinoic acid receptor beta *(RARβ)* and retinol binding protein 4 *(RBP4)* in response to RDH11 modulation (Supp Figure 2B, C).

Overall, these data suggest that in a low cholesterol environment, RDH11 may act to limit cholesterol uptake and synthesis, and attenuate inflammatory and oxidative pathways. This is interesting, given the propensity of cholesterol and lipoproteins rich in polyunsaturated fatty acids (PUFA) to become oxidatively modified, which can result in inflammation, apoptosis and ferroptosis [17,18].

2.4. Hepatic RDH11 knockdown in mice is associated with modulation of lipid metabolism pathways

Having observed changes in the transcriptional regulation of cholesterol, oxidative stress and inflammatory pathways with the modulation of RDH11 in a cell system, we next wanted to assess the effect of RDH11 loss of function on hepatic lipid metabolism *in vivo*. This was achieved using systemic delivery of adeno-associated virus (AAV) 8 particles that were engineered to express either an shRNA against RDH11, or a control shRNA (shLacZ). Assessment of hepatic RDH11 protein expression at study end, 10 weeks post-injection, demonstrated a ~60% reduction in mice receiving AAV8-shRDH11 compared to control mice ($p < 0.01$; Figure 4A). No difference in body weight at study end was observed between mice receiving shRDH11 or control vector (Figure 4B). Similarly, liver weight relative to body weight, and liver H&E staining were not significantly different between control and shRDH11 treated mice (Figure 4C and Supp Figure 3A). Attenuation of hepatic RDH11 expression resulted in significant changes in the expression of genes linked to lipid metabolism and ER stress (Figure 4F and G). We observed no effect of RDH11 knockdown on *Ldlr, Hmgcr* or *Abca1* mRNA expression (Figure 4D). We further investigated whether alternate lipid metabolic pathways such as the *de novo* lipogenesis (DNL) pathway were modulated by reduced hepatic RDH11 expression, given Brown and Goldstein demonstrated that SREBP1c, a key transcriptional regulator of triacylglycerol and fatty acid synthesis, induced RDH11 [9,19]. We observed an increase in the mRNA expression *of Acetyl-CoA carboxylase 1* (*Acaca*), the rate limiting enzyme in the DNL pathway ($p < 0.05$; Figure 4F). In addition, we investigated whether markers of oxidative stress or inflammation were upregulated, as observed with RDH11 loss of function *in vitro*. There was a trend for an increase in *Gpx3, Gpx4* and *AP-1* mRNA expression in the livers of mice receiving AAV:shRDH11 compared to control mice, similar to that observed *in vitro* in low cholesterol conditions (Figure 4G). Moreover, mRNA expression of *DNA damage inducible transcript 3* (*Ddit3;* also known as *Chop*), a marker of endoplasmic reticulum (ER) stress, was increased with RDH11 knockdown, compared to control mice (Figure 4G; $p < 0.01$). To specifically probe whether RDH11 knockdown in the liver modulated retinol metabolic pathways - a previously demonstrated function of RDH11, we performed RNA-seq and gene set enrichment analysis on livers from KD mice. The pathways most enriched in this analysis were ascorbate and aldarate metabolism (Supp Figure 3B). Whilst retinol metabolism was modestly enriched, this was predominantly driven by only two genes *Cyp2* and *Ugt* (Supp Figure 3C). Additionally we measured gene expression by qPCR and observed a significant increase in mRNA expression of lecithin retinol acyltransferase (Lrat; $p < 0.05$; Supp Figure 3D) in mice administered AAV:shRDH11; however, no significant changes were observed in expression of other genes associated with retinol metabolism (*Bco1, Bco2, Rarb, Rbp4*) as measured by qPCR (Supp Figure 3D), consistent with the *in vitro* studies. Together, these data suggest that a reduction of RDH11 drives an environment with elevated cholesterol abundance associated with increased oxidation and ER stress, which is not likely related to major alterations in retinol metabolism pathways in the liver.

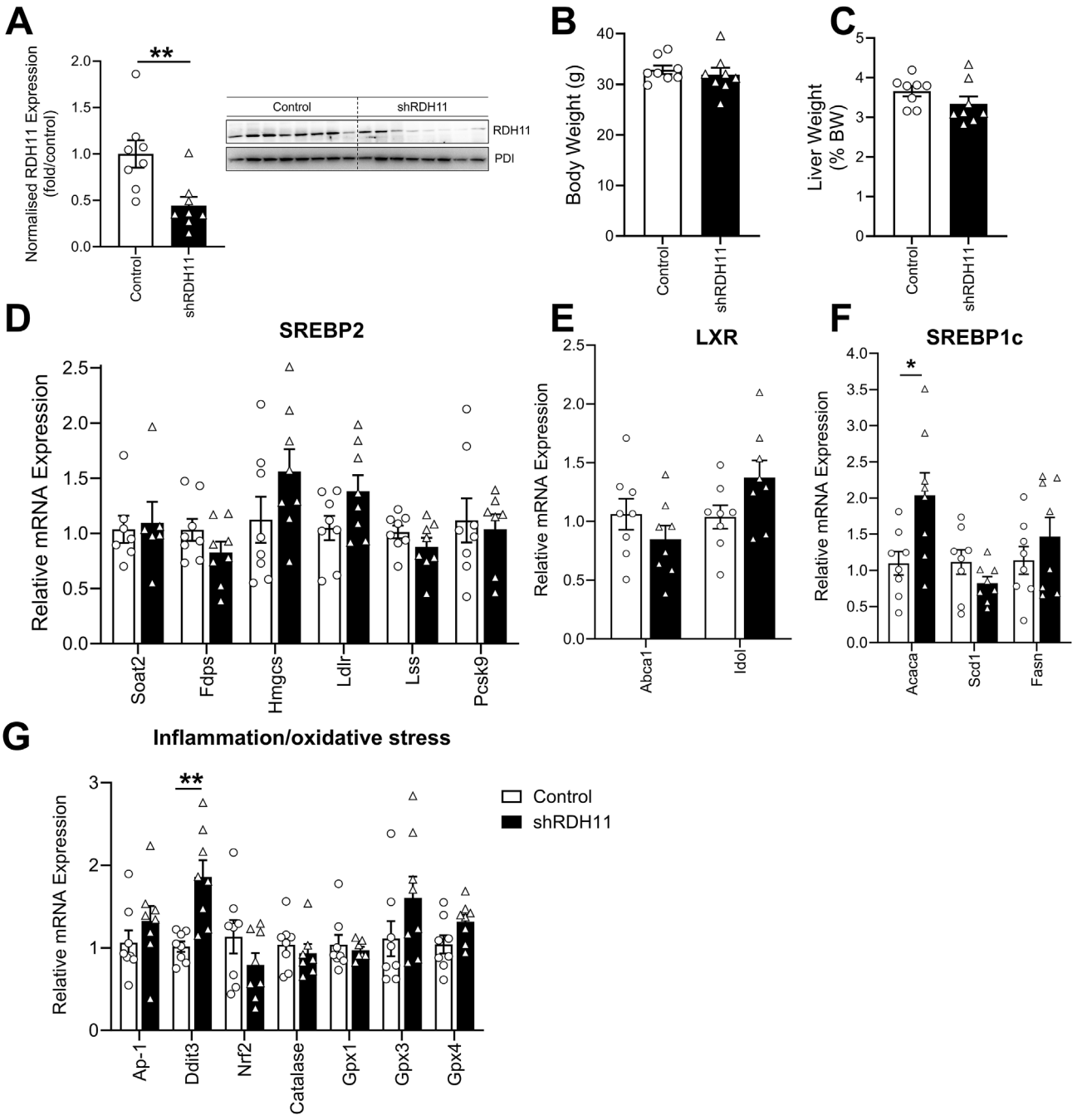

Figure 4: Attenuation of hepatic retinol dehydrogenase 11 in mice is associated with modulation of markers of lipid metabolism and endoplasmic reticulum stress (**A**) Immunoblot of RDH11 expression and loading control (PDI) and quantitation, (**B**) body weight, (**C**) liver weight normalised to body weight, (**D-F**) hepatic mRNA expression of (**D**) sterol regulatory element binding protein (SREBP)-2, (**E**) liver X receptor (LXR) and (**F**) SREBP-1c target genes and (**G**) genes linked to inflammation, endoplasmic reticulum stress and oxidative stress in C57BL/6J mice examined 10 weeks after administration of Adeno-Associated viral vector (AAV8)-shLacZ (control) or AAV8-shRDH11; RDH11, retinol dehydrogenase 11; PDI, protein disulfide isomerase; Soat2, acetyl-CoA acetyltransferase 2; Fdps, farnesyl diphosphate synthase; Hmgcs, 3-hydroxy-3-methyl-glutaryl-coenzyme A synthase; Ldlr, low density lipoprotein receptor; Lss, lanosterol synthase; Pcsk9, proprotein convertase subtilisin/kexin type 9; Abca1, ATP binding cassette transporter A1; Idol, inducible degrader of the low density lipoprotein receptor; Acaca, acetyl-coa carboxylase alpha; Scd1, stearoyl-CoA desaturase; Fasn, fatty acid synthase; Ap-1, activator protein 1; Ddit3, DNA damage-inducible transcript 3; Nrf2, nuclear factor erythroid 2-related factor 2; Cata, catalase; Gpx, glutathione peroxidase; ($n = 7–8$/group); Data presented as mean ± SEM and analysed by unpaired t-test (**A-G**) or Mann Whitney test (**F, G**); *$p < 0.05$, **$p < 0.01$.

2.5. Mice with attenuated hepatic RDH11 expression have an altered liver lipid profile

Given the impact of RDH11 on cholesterol metabolism pathways identified above, we next investigated the effect of modulating RDH11 expression on hepatic and plasma lipid abundance. We performed targeted lipidomics, which quantified over 700 individual lipid species in the liver and plasma of mice treated with AAV:shRDH11 and control vector. Whilst shRDH11 treated mice exhibited no difference in total hepatic lipid burden, the majority of the 64 individual liver lipid species that were significantly altered in abundance between control and

shRDH11 mice were increased (75%) ($p < 0.05$; Supp Figure 3E). After Benjamini Hochberg FDR correction none of these individual lipid species were significantly altered, further supporting a modest effect on the total hepatic liver burden in RDH11 suppressed mice. Probing the lipidomics more comprehensively, mice treated with shRDH11 exhibited a trend towards an increase in hepatic cholesterol esters (CEs; Figure 5A) and a significant increase in free cholesterol (COH; $p < 0.05$; Figure 5B). Given the variability in the knockdown of RDH11, we investigated whether there was a significant correlation between CEs or COH and the residual expression of hepatic RDH11. CEs were not significantly correlated with hepatic Rdh11 protein expression (Figure 5C), however COH was strongly negatively correlated with

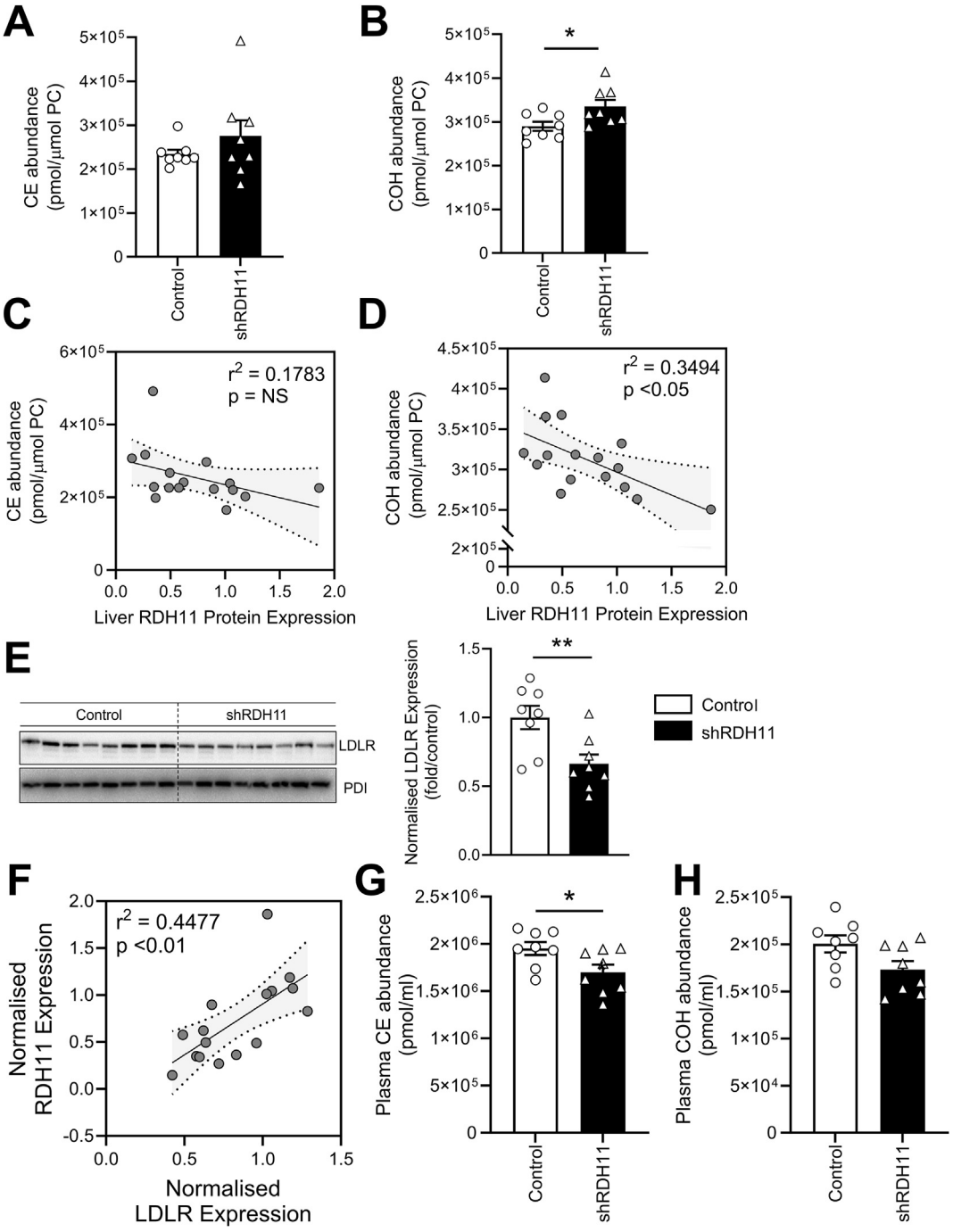

Figure 5: Attenuation of hepatic retinol dehydrogenase 11 in mice is associated with modulation of hepatic and plasma cholesterol abundance (A) Hepatic CE and (**B**) COH abundance; Pearson's correlation between hepatic RDH11 protein expression and hepatic **(C)** CE or **(D)** COH abundance; **(E)** immunoblot and quantitation of hepatic LDLR expression and loading control (PDI); (**F**) correlation between hepatic RDH11 and LDLR protein expression; plasma **(G)** CE and **(H)** COH abundance in C57BL/6J mice examined 10 weeks after administration of Adeno-Associated viral vector (AAV8)-shLacZ (control) or AAV8-shRDH11; CE, cholesterol ester; COH, free cholesterol; RDH11, retinol dehydrogenase 11; LDLR, low density lipoprotein; PDI, protein disulfide isomerase; Data presented as mean ± SEM (**A, B, E, G, H;** n = 8/group) and analysed by unpaired t-test (**B, E, G, H**), Mann Whitney test (**A**) or Pearson correlation with dotted lines representing the 95% confidence interval (**C, D, F;** n = 16) *$p < 0.05$, **$p < 0.01$.

RDH11 protein abundance (Figure 5D). These data are consistent with an increase in the ER stress marker, *Ddit3* (Figure 4G) given that COH accumulation can lead to toxicity in the liver [20]. Furthermore, hepatic LDLR protein expression was significantly reduced in shRDH11 mice ($p < 0.01$; Figure 5E), and a significant correlation between LDLR and RDH11 protein expression was observed ($p < 0.01$; Figure 5F). This is likely a response to the increased cholesterol abundance observed in the livers of shRDH11 treated mice. In contrast to that observed in the liver, we saw a significant decrease in plasma CEs ($p < 0.05$; Figure 5G) and a trend for a decrease in plasma COH ($p = 0.0511$; Figure 5H), demonstrating that attenuation of hepatic RDH11 expression impacts on systemic cholesterol metabolism. Further analysis of the hepatic lipidome revealed that phospholipids, the principal structural component of cell membranes, were also altered in relative (Figure 6A) and absolute (Supp Figures 4A) abundance between control and shRDH11 mice. Total phosphatidic acid (PA) species exhibited the most significant magnitude of change between control and shRDH11 mice, with a ~40% increase ($p < 0.01$), an effect also observed with *in vitro* RDH11 loss of function studies ($p < 0.05$; Figure 6B; Supp Table 4). Additionally, lysoalkenylphosphatidylcholine (LPC(O), alkylphosphatidylethanolamine (PE(O)) and lysophosphatidylinositol (LPI) were moderately increased ($p < 0.05$: Figure 6A; Supp Figure 4A). Whereas phosphatidylethanolamine (PE) was decreased in shRDH11 mice compared to control ($p < 0.05$; Figure 6A; Supp Figure 4A). These findings suggest that reduced RDH11 expression may impact on plasma membrane composition, which could adversely affect organelle function including ER and mitochondria.

2.6. Knockdown of hepatic RDH11 modulates markers of mitochondrial function

Given that we proposed that RDH11 may participate in the management of lipid oxidation in response to cellular cholesterol status, in addition to the differences observed in PA abundance, we next investigated the impact of RDH11 silencing on markers of mitochondrial composition and function. Firstly, we examined lipid species enriched in mitochondrial membranes, including cardiolipins, to determine whether mitochondrial structure was deleteriously altered [21]. Mice receiving AAV:shRDH11 exhibited a significant decrease in the most abundant cardiolipin (CL) species, CL 18:2_18:2_18:2_18:2 ($p < 0.05$; Figure 7A), but no major change in other less abundant CL species (Supp Figure 4B, Supp Table 5), suggestive of a remodelling in mitochondrial membrane architecture.

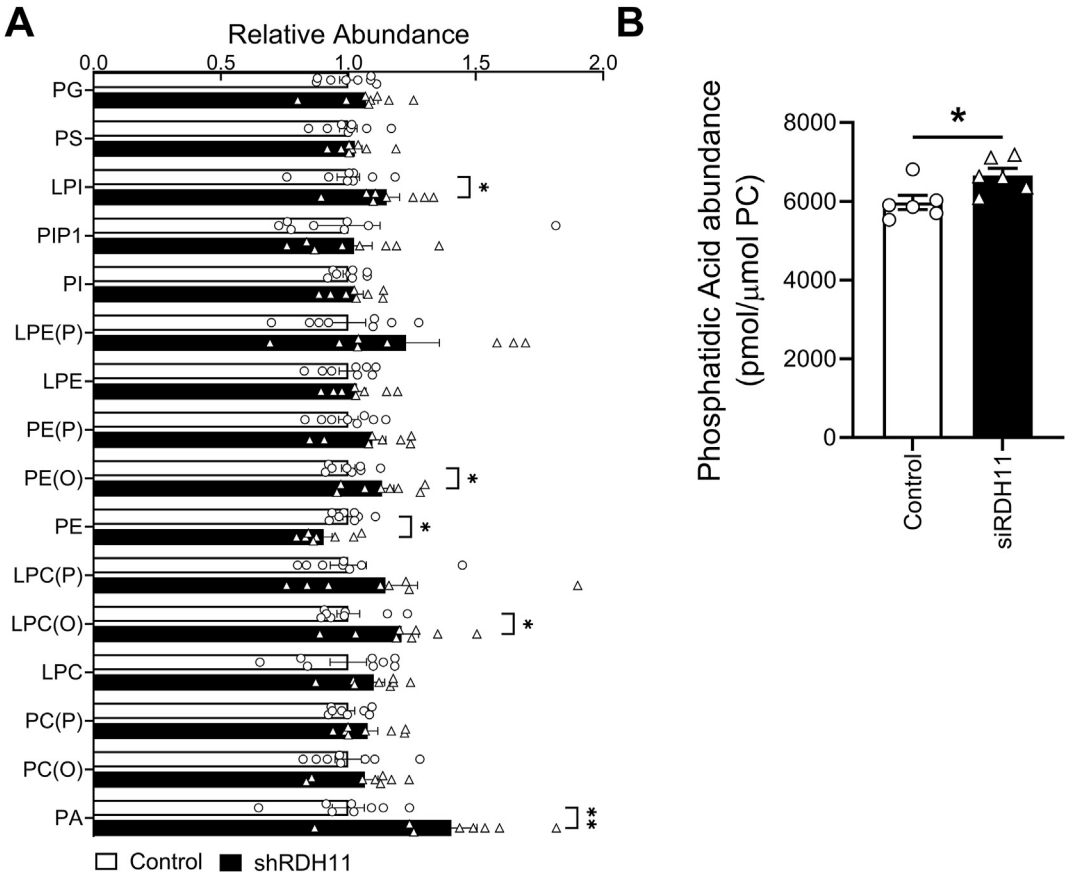

Figure 6: Attenuation of hepatic retinol dehydrogenase 11 in mice and cells is associated with modulation of phospholipid abundance (**A**) Relative abundance of hepatic phospholipid classes in C57BL/6J mice examined 10 weeks after administration of adeno-associated viral vector (AAV8)-shLacZ (control) or AAV8-shRDH11; (**B**) Total PA abundance in cells transfected with scramble siRNA (control) or siRNA RDH11 for 24 h followed by exposure to a low cholesterol (LPDS+5 μM compactin + 50 μM mevalonate) environment; PG, phosphatidylglycerol; PS, phosphatidylserine; LPI, lysophosphatidylinositol; PIP1, phosphatidylinositol-phosphate; PI, phosphatidylinositol; LPE(P) lysoalkenylphosphatidylethanolamine; LPE, lysophosphatidylethanolamine; PE(P) alkenylphosphatidylethanolamine; PE(O), alkylphosphatidylethanolamine; PE, phosphatidylethanolamine; LPC(P), lysoalkenylphosphatidylcholine; LPC(O), lysoalkylphosphatidylcholine; LPC, lysophosphatidylcholine; PC(P), alkenylphosphatidylcholine; PC(O), alkylphosphatidylcholine; PA, phosphatidic acid; PC, phosphatidylcholine. Data presented as mean ± SEM (**A**, n = 8/group; **B**, n = 6/group); Data analysed by unpaired t-test *$p < 0.05$, **$p < 0.01$.

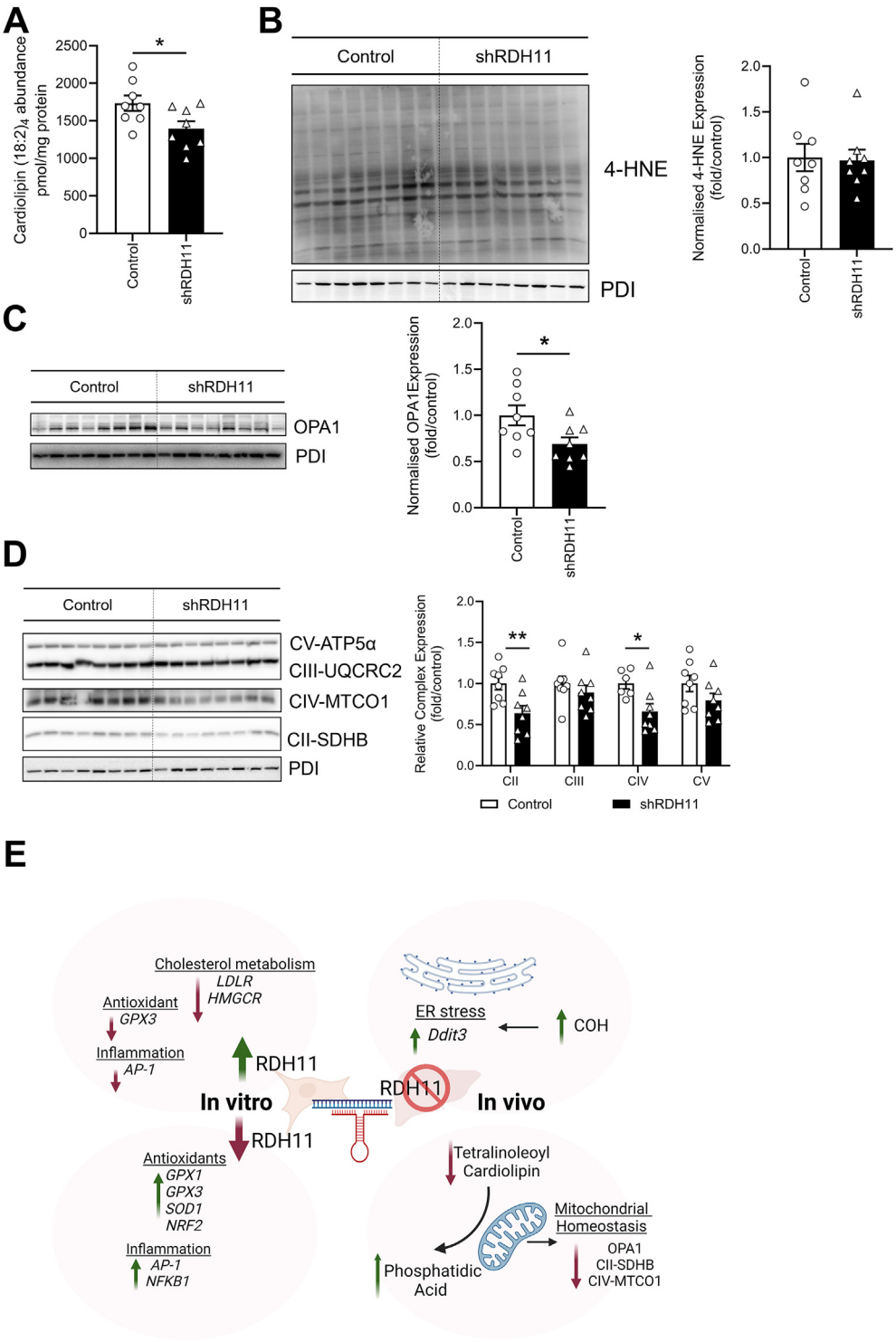

Figure 7: Attenuation of hepatic retinol dehydrogenase 11 alters mitochondrial lipids and proteins (A) Cardiolipin $(18:2)_4$ abundance, **(B)** immunoblot and quantitation of 4-HNE and loading control (PDI), (**C**) immunoblot and quantitation of OPA1 and loading control (PDI), **(D)** immunoblot and quantitation of complex II (CII; SDHB), complex III (CIII; UQCRC2), complex IV (CIV; MTCO1) and complex V (CV; ATP5a) and loading control (PDI) in livers of C57BL/6J mice examined 10 weeks after administration of Adeno-Associated viral vector (AAV8)-shLacZ (control) or AAV8-shRDH11; (**E**) Schematic of the hypothesized role of RDH11 in the liver; 4-HNE, hydroxynonenal; PDI, protein disulfide isomerase; OPA1, mitochondrial dynamin like GTPase; SDHB, succinate dehydrogenase complex iron sulfur subunit B; UQCRC2, ubiquinol cytochrome c reductase core protein 2; MTCO1, mitochondrially encoded cytochrome c oxidase I; ATP5a, ATP synthase subunit alpha; *AP-1*, activator protein 1; *Ddit3*, DNA damage-inducible transcript 3; *GPX*, glutathione peroxidase; *HMGCR*, 3-hydroxy-3-methyl-glutaryl-coenzyme A reductase; *LDLR*, low density-lipoprotein receptor; *NFKB1*, nuclear factor NF-kappa-B1; *NRF2*, nuclear factor erythroid 2-related factor 2; *RDH11*, retinol dehydrogenase 11; *SOD1*, superoxide dismutase 1; (**A-D**) Data presented as mean ± SEM (n = 6–8/group) and analysed by unpaired t-test; *p < 0.05, **p < 0.01.

As perturbed mitochondrial function has been shown to impact on the production of reactive oxygen species (ROS) [22], we sought to investigate whether a reduction in hepatic RDH11 expression was associated with increased production of lipid peroxidation products such as 4-hydroxynonenal (4-HNE) adducts. We observed no difference in 4-HNE adducts in the liver of mice administered AAV:shRDH11 (Figure 7B), which may be due in part to a compensatory upregulation of antioxidant enzymes, given the trend for an upregulation of *Gpx* family members observed in these mice (Figure 4G). Lastly, given that the electron transport chain (ETC) complexes as well as optic atrophy 1 mitochondrial dynamin like GTPase (OPA1) have been shown to be modulated by cardiolipin abundance, we investigated the abundance of these proteins in the livers of shRDH11 and control treated mice [23]. We observed a significant decrease in OPA1, a key protein important in inner mitochondrial membrane fusion ($p < 0.05$; Figure 7C), with attenuation of RDH11. We also measured the expression of components of the mitochondrial ETC. Complex II (SDHB) and complex IV (MTCO1) were significantly decreased in shRDH11 mice ($p < 0.01$ and $p < 0.05$, respectively; Figure 7D). Taken together, these data suggest that a reduction in hepatic RDH11 is associated with modulation of cholesterol metabolism pathways, resulting in the increased abundance of hepatic free cholesterol, as well as numerous PUFA containing phospholipids that are prone to oxidation, resulting in a concomitant increase in ER stress and markers of mitochondrial dysfunction. These observations present evidence for RDH11 being an important protein at the crossroads of hepatic lipid metabolism and cellular redox homeostasis (Figure 7E).

3. DISCUSSION

Here, we utilised a systems genetics discovery platform to identify novel proteins associated with the regulation of hepatic cholesterol regulation. This approach demonstrated that RDH11 significantly correlated with numerous proteins known to play a role in the regulation of cholesterol metabolism. Subsequent study of RDH11 demonstrated that it is transcriptionally responsive to altered cholesterol environments. Furthermore, gain- and loss-of function experiments support an effect of RDH11 on the expression of key regulators of cholesterol metabolism, as well as inflammatory and oxidative pathways. Likewise, hepatic RDH11 knockdown in mice significantly altered markers of lipid metabolism, with a consequent modulation of hepatic lipid accumulation. Specifically, we observed an increase in hepatic free cholesterol and phosphatidic acid and a decrease in cardiolipin abundance, with consequent changes in markers of ER stress and mitochondrial function. Such changes may have implications for cell membrane structure and signalling, redox status and mitochondrial homeostasis.

Previous studies characterising the localisation of RDH11 have demonstrated that it is highly concentrated at the endoplasmic reticulum (ER) [7]. Indeed, the bulk of the cellular enzymatic machinery devoted to cholesterol synthesis under the transcriptional regulation of sterol response element binding protein 2 (SREBP2) is similarly localised to the ER. This co-localisation suggests a shared or complementary function between RDH11 and regulators of cholesterol synthesis. We demonstrated that RDH11 is transcriptionally regulated by cholesterol abundance, in a manner consistent with other SREBP2 targets; an effect that appears to be conserved in both mice and humans. This concept is consistent with the findings of Brown and Goldstein, who previously demonstrated that the mouse homologue of RDH11, which they named SCALD (short chain aldehyde dehydrogenase), was transcriptionally regulated not only by SREBP2, but also SREBP1a and SREBP1c [9].

Endogenous hepatic cholesterol regulation is finely controlled, and it is therefore not surprising that the management of oxidative by-products associated with the synthesis of cholesterol, forms part of its complex regulatory framework. Ectopic expression of RDH11 was associated with an attenuation of LDLR and HMGCR expression in low cholesterol conditions *in vitro*, consistent with diminished cholesterol synthesis and uptake. In agreement with the hypothesis put forward by Brown and Goldstein, we postulate that RDH11 could play a role in protecting the cell from excess cholesterol, which can be prone to oxidative attack from ROS [9]. Indeed, type 1 autoxidation of cholesterol, whereby the molecule undergoes non-enzymatic oxidation due to free radical attack, can generate significant amounts oxysterols as seen in circulating oxidised LDL particles [24]. Previous reports have demonstrated that oxidised cholesterols and free cholesterol can drive membrane dysfunction, leading to inflammation and apoptosis [17,18]. This hypothesis is further supported by our findings that demonstrated that attenuation of RDH11 was associated with an increase in the abundance of hepatic free cholesterol *in vivo* and an increase in the ER stress marker, Ddit3. Consistent with the abovementioned hypothesis, the absence of RDH11 was associated with an increase in markers of inflammation *in vitro*.

Further to modulating cholesterol synthesis, SREBPs promote the synthesis, elongation, desaturation, and uptake of polyunsaturated fatty acids (PUFA) [19]. We provide evidence that RDH11 may play a broader role in lipid metabolism and not just exclusively cholesterol homeostasis. We observed that ectopic expression of RDH11 was associated with an attenuation of LDLR expression *in vitro*. Equally, loss of RDH11 *in vivo* was associated with an increase in expression of *Acaca*, the rate limiting enzyme in the DNL pathway, thus limiting the uptake and synthesis of fatty acids. Furthermore, given that uptake of PUFA-rich lipoproteins by the LDLR delivers lipid that are susceptible to lipid peroxidation, which can form peroxides and fatty aldehydes such as 4-HNE, we speculate that RDH11 may also act to reduce aberrant PUFA peroxidation, consistent with the hypothesis of Kasus-Jacobi et al., that proposed RDH11 may be induced to convert these toxic aldehydes into non-toxic alcohols [9]. More recently, it was demonstrated that HEK293 cells stably expressing murine RDH11 were protected against 4-HNE modification and 4-HNE-induced apoptosis [25]. In contrast, in the mouse retina, RDH11 is not necessary or likely, to be playing a direct role in reacting with these toxic aldehyde species [25]. Further to this, retinal RDH11 was not induced upon exposure to oxidative stress associated with light exposure [14]. It therefore remains unclear as to how RDH11 mechanistically contributes to the management of lipid peroxidation products and whether the role of RDH11 is conserved across tissues and cell types. Our studies focused on characterising RDH11 function in the liver and hepatocytes. *In vitro,* RDH11 loss-of-function was associated with an upregulation of markers of inflammation, NFκB1, and AP-1 as well as an increase in modulators of anti-oxidative pathways, GPX1, GPX3, SOD1 and NRF2 in low cholesterol conditions, a setting in which upregulation of cholesterol biosynthesis and uptake occurs. These changes suggest a significant compensatory mechanism exists to limit the amount of ROS [26] in the absence of RDH11, and could explain why we did not observe changes in the abundance of 4-HNE. Likewise, we previously reported in a post-developmental, skeletal muscle specific SOD2 KO model, that mice exhibited only a subtle decrease in muscle 4-HNE abundance and a concomitant increase in catalase as well as GPX1, 3 and 4 mRNA expression [27]. These results may be explained by the fact that numerous cellular mechanisms exist to manage oxidative stress including enzymatic proteins SOD, catalase and GPX [26] as well as through non-enzymatic means such as glutathione and coenzyme Q10.

A key finding from these studies is the modulation of phospholipid species in both cells and mice with reduced RDH11. Briefly, all phospholipids comprise of a phosphate head group and contain 2 fatty acyl chains. These fatty acyl chains are predominately unsaturated which facilitates membrane fluidity, although this renders these fatty acids susceptible to peroxidation [28]. Phosphatidic acid (PA) levels were significantly elevated in our RDH11 loss-of-function mouse and cell models. PAs are the simplest phospholipids, and contribute to intracellular signalling as well as promoting negative membrane curvature, which is required for plasma membrane structure. In addition, PAs act as a substrate for more complex lipids including cardiolipins, a tetrameric lipid highly concentrated in the inner mitochondrial membrane. One possible explanation for the increase in PA could be the fragmentation of cardiolipin into PA, an effect that can occur under conditions of oxidative stress [29]. Indeed, we observed a concomitant reduction in the abundance of the predominant cardiolipin species, tetra linoleoyl cardiolipin ($18:2_4$). A key function of cardiolipins is to stabilise mitochondrial membranes to facilitate the ETC, and alterations in cardiolipin abundance can impact complex stability and activity [30–32]. Consistent with this, we observed a significant reduction in the expression of complexes II and IV of the ETC and in the mitochondria dynamics protein, OPA1, suggesting perturbations to mitochondrial homeostasis, perhaps modulated by changes in cardiolipin abundance.

Our data provide evidence that RDH11 gain- and loss-of- function modulates metabolic effects independent of the RXR/retinoid metabolism pathway. In contrast, previous studies in human epidermal skin-rafts have demonstrated that RDH11 is responsive to all-trans-retinoic acids (ATRA) [33]. Intriguingly, the more studied family member RDH10, was responsive to ATRA in epidermal rafts. This effect was also observed in HEK293 cells, but not human liver HepG2 cells, supporting cell-type specific actions of retinol dehydrogenases. Similarly, RDH11 appears to be involved in retinol homeostasis in a tissue-specific manner *in vivo*. RDH11 null mice fed a diet with reduced Vitamin A exhibited no change in retinol levels in the liver, but a trend for a reduction in the testes compared to wild type (WT) mice [34]. However, RDH11 null mice fed a Vitamin A deficient diet exhibited significantly reduced retinols in both the liver and testes compared to WT mice [34], indicating that RDH11 may have some function in retinol metabolism, albeit under profound nutrient restriction.

A limitation to the current study was the lack of knockdown efficiency in our mouse model, with a ~60% attenuation of hepatic RDH11 protein expression observed. Expression was driven by a CMV promoter using a synthetic inhibitory BIC/miR-155 RNA backbone to induce shRNA expression. Moreover, we used an AAV8 serotype, which has a high affinity and transduction efficiency for hepatocytes. Given this, possible explanations for the lack of knockdown efficiency include (i) the shRNA sequence directed against RDH11 had off-target effects; (ii) cell populations in the liver other than hepatocytes were contributing to total hepatic RDH11 expression or (iii) regeneration of hepatocytes reduced RDH11 knockdown over time, although this is unlikely to be a major contributing factor in this timeframe [35]. Generation of a conditional knockout using conventional methods such as cre-lox targeting hepatocytes via the albumin promoter would have allowed us to characterise the effect of loss of hepatocyte-specific RDH11 more robustly on cholesterol metabolism and its downstream effects, however this may have resulted in further compensatory effects. Another limitation is the conditions under which we studied the mice. Mice were fed a chow diet which is deficient in cholesterol, mimicking a 'low-cholesterol' environment, an *in vitro* setting in which we saw the greatest effects of RDH11; however, it is possible that greater effects may have been seen in a setting such as fasting/re-feeding, in which there is robust activation of the SREBP, and indeed the DNL pathway [36]. Nevertheless, to the best of our knowledge, this is the most in-depth experimental validation study describing a role for RDH11 in the context of hepatic cholesterol metabolism, with implications for the regulation of lipid metabolism and downstream effects on oxidative, inflammatory, and mitochondrial pathways in mammals.

4. METHODS

4.1. Hybrid mouse diversity panel platform and pathway analysis

Co-correlation analysis of hepatic protein abundance across strains of the hybrid mouse diversity panel (HMDP) was performed on proteomic data published by our group previously [6]. Pathway enrichment analysis was performed using the Shiny GO v0.8 developed and maintained by the South Dakota State University [37]. Target lists were generated from proteins that significantly correlated with RDH11 across the HMDP, then entered as a gene list into the Shiny GO query. Background adjustment was enabled against all detectable proteins (8370 proteins) in the initial HMDP analysis and then entered as a gene list. Bulk RNAseq data from the RDH11 mouse study was entered as the list of significantly differentially expressed liver transcripts with background adjustments against all detectable transcripts. Functional annotation clustering of KEGG pathways was performed with default settings. Only clustered annotated terms that were significant after FDR adjustment $q < 0.05$ were included. KEGG pathway diagrams [38,39] were also derived though Shiny GO webapp.

4.2. Cell culture and *in vitro* studies

Human hepatoma (Hep3B) cells were obtained from American Type Culture Collection (ATCC). Cells were maintained in high glucose Dulbecco's Modified Eagle Medium (DMEM; Thermofisher), supplemented with 10% foetal bovine serum (FBS; Gibco) and 1% sodium pyruvate (Sigma Aldrich). Cells were passaged for experimental use to a maximum of 20 times before being discarded and were periodically tested for mycoplasma contamination. For cholesterol modulation experiments, cells were treated with either 10% FBS (full serum, FS) or 10% Lipoprotein Deficient Foetal Bovine Serum (LPDS) in DMEM with the addition of cholesterol modulating agents, as indicated. The following cholesterol modifying agents were added: 5 μM compactin (statin; Sigma Aldrich) dissolved in dimethyl sulfoxide (DMSO; Sigma Aldrich) plus 50 μM mevalonate (Sigma Aldrich) dissolved in ethanol (Thermofisher); 20 μM 25-hydroxycholesterol (25HC; Sigma Aldrich) plus vehicle (0.1% DMSO), 20 mg/ml methyl-β-cyclodextrin (CD; Sigma Aldrich) plus vehicle (0.1% DMSO and 0.02% ethanol), 20 mg/ml cholesterol loaded methyl-β-cyclodextrin (Chol/CD) plus vehicle (0.1% DMSO and 0.02% ethanol) or 10 μm T0901317 (T0; Sigma Aldrich) plus vehicle (0.02% ethanol). For add-back experiments cells were treated with either 10% FBS DMEM or LPDS DMEM plus 5 μM compactin and 50 μM mevalonate for 24 h, followed by either a further 24 h in LPDS DMEM with compactin and mevalonate alone, or with the addition of 5 mg/ml low-density lipoprotein cholesterol (LDL-C) (kind gift from Professor Dmitri Sviridov, Baker Institute) or 20 μM 25HC. At the experimental endpoint, cells were washed in ice cold PBS without Ca^{2+}/ and Mg^{2+}.

4.3. Cloning

The *RDH11* gene sequence was amplified from Hep3B cDNAs using Phusion DNA polymerase (Thermofisher). The following Gateway primers were used: *F Primer-GGGGACAAGTTTGTACAAAAAAGCAGGCT*

TTGCCACCATGGTTGAGCTCATGTTCCCGCTG and R Primer-GGGACCA CTTTGTACAAGAAAGCTGGGTTTTAGTCTATTGGGAGGCCCAGCAGG. The *RDH11* cDNA sequence was shuttled into pcDNA3.1 vector using gateway technology (Thermofisher) [40]. The expression vector was sequence verified (Micromon, Monash Clayton) and subsequently purified (Promega) before *in vitro* use.

4.4. Animal studies

Male C57BL/6J mice were housed at the Alfred Research Alliance Animal Service facility. Animals were housed at 22 °C on a 12hr light/dark cycle with *ad libitum* access to food (rodent chow, Specialty Feeds, Australia) and water, with cages changed weekly. For diet studies, at 8 weeks of age, mice were fed either a chow diet, high fat diet (HFD; SF00-219, Specialty Feeds, Australia) or Western Diet (WD; SF04-001, Specialty Feeds, Australia) for 16 weeks. For the statin study, at 8 weeks of age, mice received vehicle or simvastatin (100 mg per kg^{-1}; Sigma Aldrich) by gavage daily for 2 weeks. For the RDH11 study, at 8 weeks of age mice were administered an adeno-associated virus serotype 8 (AAV8) containing two short hairpin RNA sequences targeting *Rdh11,* or *LacZ* (control) via tail vein injection (5×10^{10} vg; n = 8/group). RDH11 sequences: shRNA 1—5′-CCGG-CAAGGTCG-CAATGAGATAATA-CTCGAG-TATTATCTCATTGCGACCTTG-TTTTTG-3′ and shRNA 2—5′-CCGG-TCACTTCCTCCTGACCCATTT-CTCGAG-AAATGGGTCAGGAGGAAGTGA-TTTTTG-3'. At the study endpoint, mice were fasted for 4 h prior to being anesthetised and euthanased via exsanguination and blood and tissues collected and stored at −80 °C for further analysis. All procedures and protocols were compliant with the Alfred Research Alliance Animal Ethics Committee.

4.5. Primary mouse hepatocyte isolation

Mouse primary hepatocytes were isolated from 6-week-old male C57BL/6J mice. Mouse livers were perfused via the inferior vena cava with Hanks' Balanced Salt solution (HBSS) (Merck) with 0.5 mM EDTA. Upon perfusion (50—80 ml HBSS), Collagenase A (Sigma) in HBSS and 5 mM $CaCl_2$ was then perfused to digest the liver until pale in colour (50—60 ml). The liver was then dissected and placed in HBSS to collect released hepatocytes. Hepatocytes were filtered twice through a 250 μm nylon mesh, washing with HBBS. The hepatocyte suspension was centrifuged at 50 g for 2 min then HBSS was aspirated. The remaining pelleted cells were then resuspended in HBSS and centrifuged at 50 g for 2 min. HBSS was aspirated for a final time leaving the cell pellet. Cells were resuspended in M199 media (Gibco) and passed through a 250 μm nylon mesh to remove debris. Cell viability was assessed with 0.4% trypan blue (Thermo Fisher). Viability above 70% was considered appropriate for downstream experimental use. Experiments were performed as above for Hep3B add back experiments.

4.6. RNA extraction and qPCR

Harvested cells or frozen tissue were homogenised in RNAzol (in house preparation) on ice. 50 μl of 1—bromo—3—chloropropane (BCP) for cell preparations, or 100ul of chloroform for liver samples, was added to phase separate RNA. RNA was precipitated in isopropanol at room temperature, pelleted and washed in ice cold 75% (v/v) ethanol. RNA was quantified and assessed for purity using a Nanodrop 2000c spectrophotometer (Thermo Fisher Scientific). RNA was reverse transcribed into cDNA (Applied Biosystems Veriti PCR Machine) and diluted in water to 5 ng/ul. 10 ng of cDNA was added to SYBR Green master mixes containing sequence specific primers (Supp Table 1) for analysis by quantitative real-time PCR (qPCR). Samples were run on the Applied Biosystems QuantStudio 7 Flex Real-Time PCR System with a 384-well plate reader. Raw expression data was normalised to the house keeping genes ribosomal protein lateral stalk subunit P0 (RPLP0; cell experiments) or peptidylprolyl isomerase A (PPIA; animal studies) and expressed relative to the control group using the $2^{-\Delta\Delta CT}$ method [41].

4.7. Protein extraction

For *in vitro* experiments cells were washed twice with ice cold PBS without Ca^{2+} and Mg^{2+} to remove residual media. Ice cold Radio Immunoprecipitation Assay (RIPA) lysis buffer containing 1% (v/v) RIPA (0.5M Tris-HCl, pH 7.4, 1.5M NaCl, 2.5% deoxycholic acid, 10% nonyl phenoxypolyethoxylethanol, 10 mM EDTA),10% (v/v) protease inhibitor cocktail (PIC), 1 mM EDTA, 100 μM PMSF, 1 mM β-glycerophosphate, 1 mM NaF, 1 mM Sodium orthovanadate and, 2.5 mM Sodium pyrophosphate was added to each well (100—150 μl) and cells were then scraped to mechanically dislodge and disrupt cell membranes. Frozen mouse liver pieces were homogenised in ice cold RIPA lysis buffer (200—300 μl) as described above, using a motorised pestle homogeniser. Samples were rotated for 1 h at 4 °C prior to centrifugation at 10,000 g for 10 mins at 4 °C to pellet cell debris. Supernatant was collected and assayed to determine protein concentration using either a Bradford protein assay or Pierce™ BCA Protein Assay Kit (Thermo Fisher Scientific) following the manufacturers protocol.

4.8. Immunoblotting

Equal amounts of protein were resolved by SDS-PAGE on a 10% or 12% separating gel before being transferred onto polyvinylidene difluoride (PVDF) membranes, blocked in 3% (w/v) skim milk in TBS and incubated overnight with the following primary antibodies: 4-HNE (Abcam), Total OXPHOS Rodent WB Antibody Cocktail (Abcam), OPA1 (Cell signalling), LDLR (Cayman), RDH11 (Origene) or PDI (Cell signalling). The following day membranes were washed, and mouse or rabbit IgG secondary horseradish peroxidase conjugated antibodies (Santa Cruz) were added in 3% (w/v) skim milk. Membranes were imaged on either the ChemiDoc or ChemiDoc XRS (Biorad). Band visualisation was determined using Supersignal™ West Pico Chemiluminescent Substrate and Supersignal™ West Femto Chemiluminescent (Thermo Fisher Scientific). ImageLab 6.0.1 (BioRad) was used to perform normalisation and densitometry.

4.9. Lipidomics

Briefly, frozen liver tissue or lysed cells were homogenised on ice in 200—400 μl PBS without Ca^{2+} and Mg^{2+}. Following homogenisation, samples were sonicated twice at 25 amps for 10 s to ensure a uniform homogenate. Protein concentrations of samples were analysed using the Pierce BCA protein assay kit, following the manufacturer's protocol. All samples were extracted as previously described [42]. Briefly, cell and liver samples were diluted with PBS, so the final concentration was 50ug protein in 10ul homogenate. For plasma, 10 μl was aliquoted using a positive displacement pipette, directly into the extraction tubes. Following sample preparation, 10 μl of pooled lipid standard (ISTD) was added to normalise lipid values for each individual sample. Lipids were extracted in 200 μl chloroform/methanol (2:1). Samples were reconstituted in 50 μl water saturated butanol and 50 μl methanol with 10 mM ammonium formate, butanol:methanol (1:1) and then centrifuged at 2000 g for 5 mins. Samples were then transferred into 0.2 ml micro inserts in 1.5 ml glass vials with Teflon insert capes in preparation for loading into the mass spectrometer. Samples, plasma quality controls (PQCs) and ISTD blanks were analysed as previously described [43] on an Agilent 6490 QQQ or Agilent 4000 (cardiolipins) mass spectrometer with an Agilent 1290 series HPLC system. Spectrometry was analysed using MassHunter Data Analysis Acquisition v 7.1 (Agilent Technologies). Results from the

chromatographic data was analysed using Mass Hunter Quantitative Analysis B9.0 where relative lipid abundances were calculated by relating each area under the chromatogram for each lipid species to the corresponding internal standard. Correction factors were applied to adjust for different response factors, where these were known. Data was normalised to total phosphatidylcholine (PC) content, total protein (cardiolipins) or volume (plasma) as indicated.

4.10. RNA sequencing (RNA-seq)

Bulk RNA sequencing was performed as previously described [44]. RNA was extracted from livers using The Direct-zol RNA MiniPrep kit according to manufacturer's instructions (Zymo Research). RNA quality for sequencing was determined using the high-sensitivity Agilent RNA ScreenTape Assay for 4200 Tape Station System (Agilent Technologies). Only samples with an RNA Integrity Number (RIN) score >9 were selected for subsequent analysis. DNA libraries were generated as per the manufacturer's protocol using the NEBNext® Poly(A) mRNA Magnetic Isolation Module kit (New England Biolabs). 1 μg total RNA per sample was inputted and adaptor ligation and PCR enrichment was performed using the NEBNext® Multiplex Oligos for Illumina® kit as per manufacturer's instructions. Libraries for each of the 9 samples were individually bar coded using n6-barcodes and library quantity and quality were assessed as per manufacturer's instructions using the Agilent D1000 ScreenTape Assay for 4200 TapeStation System. DNA libraries were pooled and then run on a NovaSeq 6000 sequencer at the Centre of Genomic Medicine at the Alfred Hospital/Monash University. Reads were performed as paired end with an average read length of 66 base pairs with an average of $>$20M reads per sample.

4.11. Histology

Cross sectional liver slices were embedded cut side down in OCT before being frozen in isopentane on dry ice. Following freezing blocks were cut into 7 μm sections using a Leica CM1950 Cyrostat. Sections were fixed on slides in 100% methanol and stained with haematoxylin and eosin. Slides were captured at 20X magnification using Zeiss Axioscan 7 (Zeiss) and images generated with QuPath open-source software.

4.12. Statistical analysis and data exclusion

Data was assessed for normality using a Shapiro—Wilk test. Normally distributed data was assessed using an unpaired t-test or a one- or two-way ANOVA (with an uncorrected Fisher's LSD post-hoc test). Non-normally distributed data was analysed using a Mann Whitney test or a Kruskal—Wallis test (with an uncorrected Dunn's post-hoc test), unless otherwise indicated. Data are presented as mean ± SEM, unless otherwise indicated. $p < 0.05$ was considered significant.
Data points were only excluded if they were identified using Tukey's outlier detection test (Q1-1.5*IQR/Q3+1.5*IQR) and deemed to have occurred as a result of a technical failure (e.g., failed amplification in qPCR), or were an outlier for 3 or more mRNA expression analyses. Animal study analyses were performed in a blinded fashion (i.e. on grouped datasets before viral vector shRNAs were known).

CREDIT AUTHORSHIP CONTRIBUTION STATEMENT

Michael F. Keating: Writing — review & editing, Writing — original draft, Project administration, Methodology, Formal analysis, Data curation, Conceptualization. **Christine Yang:** Project administration, Methodology, Investigation, Data curation. **Yingying Liu:** Methodology, Investigation, Data curation. **Eleanor AM. Gould:** Methodology, Investigation, Formal analysis, Data curation. **Mitchell T. Hallam:** Investigation, Formal analysis, Data curation. **Darren C. Henstridge:** Methodology, Investigation, Data curation. **Natalie A. Mellett:** Methodology, Investigation, Data curation. **Peter J. Meikle:** Supervision, Resources, Methodology. **Kevin I. Watt:** Methodology, Investigation, Data curation. **Paul Gregorevic:** Writing — review & editing, Supervision, Resources, Methodology. **Anna C. Calkin:** Writing — review & editing, Writing — original draft, Supervision, Project administration, Methodology, Investigation, Funding acquisition, Formal analysis, Data curation, Conceptualization. **Brian G. Drew:** Writing — review & editing, Writing — original draft, Supervision, Resources, Project administration, Methodology, Investigation, Funding acquisition, Formal analysis, Data curation, Conceptualization.

ACKNOWLEDGEMENTS

The Authors thank Dr Hongwei Qian (University of Melbourne) for producing the AAV vectors. This work was supported in part by the Victorian Government's Operational Infrastructure Support Program. PG was supported by funding from the National Health and Medical Research Council of Australia (1117835; 2017070). ACC was supported by a National Heart Foundation of Australia Future Leader Fellowship (105631).

DECLARATION OF COMPETING INTEREST

The authors declare the following financial interests/personal relationships which may be considered as potential competing interests: Brian G Drew reports financial support was provided by National Health and Medical Research Council. If there are other authors, they declare that they have no known competing financial interests or personal relationships that could have appeared to influence the work reported in this paper.

DATA AVAILABILITY

Data will be made available on request.

APPENDIX A. SUPPLEMENTARY DATA

Supplementary data to this article can be found online at https://doi.org/10.1016/j.molmet.2024.102041.

REFERENCES

[1] Luo J, Yang H, Song B-L. Mechanisms and regulation of cholesterol homeostasis. Nat Rev Mol Cell Biol 2020;21(4):225—45.
[2] Venkateswaran A, Laffitte BA, Joseph SB, Mak PA, Wilpitz DC, Edwards PA, et al. Control of cellular cholesterol efflux by the nuclear oxysterol receptor LXR alpha. Proc Natl Acad Sci USA 2000;97(22):12097—102.
[3] Brown MS, Goldstein JL. A proteolytic pathway that controls the cholesterol content of membranes, cells, and blood. Proc Natl Acad Sci USA 1999;96(20):11041—8.
[4] Kannel WB, Castelli WP, Gordon T. Cholesterol in the prediction of atherosclerotic disease. New perspectives based on the Framingham study. Ann Intern Med 1979;90(1):85—91.
[5] Parks BW, Nam E, Org E, Kostem E, Norheim F, Hui ST, et al. Genetic control of obesity and gut microbiota composition in response to high-fat, high-sucrose diet in mice. Cell Metabol 2013;17(1):141—52.
[6] Parker BL, Calkin AC, Seldin MM, Keating MF, Tarling EJ, Yang P, et al. An integrative systems genetic analysis of mammalian lipid metabolism. Nature 2019;567(7747):187—93.

[7] Kedishvili NY, Chumakova OV, Chetyrkin SV, Belyaeva OV, Lapshina EA, Lin DW, et al. Evidence that the human gene for prostate short-chain dehydrogenase/reductase (PSDR1) encodes a novel retinal reductase (RalR1). J Biol Chem 2002;277(32):28909–15.
[8] Lin B, White JT, Ferguson C, Wang S, Vessella R, Bumgarner R, et al. Prostate short-chain dehydrogenase reductase 1 (PSDR1): a new member of the short-chain steroid dehydrogenase/reductase family highly expressed in normal and neoplastic prostate epithelium. Cancer Res 2001;61(4):1611–8.
[9] Kasus-Jacobi A, Ou J, Bashmakov YK, Shelton JM, Richardson JA, Goldstein JL, et al. Characterization of mouse short-chain aldehyde reductase (SCALD), an enzyme regulated by sterol regulatory element-binding proteins. J Biol Chem 2003;278(34):32380–9.
[10] Haeseleer F, Jang GF, Imanishi Y, Driessen C, Matsumura M, Nelson PS, et al. Dual-substrate specificity short chain retinol dehydrogenases from the vertebrate retina. J Biol Chem 2002;277(47):45537–46.
[11] Medina MW, Bauzon F, Naidoo D, Theusch E, Stevens K, Schilde J, et al. Transmembrane protein 55B is a novel regulator of cellular cholesterol metabolism. Arterioscler Thromb Vasc Biol 2014;34(9):1917–23.
[12] Li H, Rukina D, David FPA, Li TY, Oh C-M, Gao AW, et al. Identifying gene function and module connections by the integration of multispecies expression compendia. Genome Res 2019;29(12):2034–45.
[13] Votava JA, John SV, Li Z, Chen S, Fan J, Parks BW. Mining cholesterol genes from thousands of mouse livers identifies aldolase C as a regulator of cholesterol biosynthesis. J Lipid Res 2024;65(3):100525.
[14] Kanan Y, Wicker LD, Al-Ubaidi MR, Mandal NA, Kasus-Jacobi A. Retinol dehydrogenases RDH11 and RDH12 in the mouse retina: expression levels during development and regulation by oxidative stress. Invest Ophthalmol Vis Sci 2008;49(3):1071–8.
[15] Shaulian E. AP-1–The Jun proteins: oncogenes or tumor suppressors in disguise? Cell Signal 2010;22(6):894–9.
[16] Deneke SM, Fanburg BL. Regulation of cellular glutathione. Am J Physiol 1989;257(4 Pt 1):L163–73.
[17] Zerbinati C, Iuliano L. Cholesterol and related sterols autoxidation. Free Radic Biol Med 2017;111:151–5.
[18] Yang WS, Kim KJ, Gaschler MM, Patel M, Shchepinov MS, Stockwell BR. Peroxidation of polyunsaturated fatty acids by lipoxygenases drives ferroptosis. Proc Natl Acad Sci USA 2016;113(34):E4966–75.
[19] Horton JD, Goldstein JL, Brown MS. SREBPs: activators of the complete program of cholesterol and fatty acid synthesis in the liver. J Clin Invest 2002;109(9):1125–31.
[20] Ioannou GN, Subramanian S, Chait A, Haigh WG, Yeh MM, Farrell GC, et al. Cholesterol crystallization within hepatocyte lipid droplets and its role in murine NASH. J Lipid Res 2017;58(6):1067–79.
[21] Ren M, Phoon CK, Schlame M. Metabolism and function of mitochondrial cardiolipin. Prog Lipid Res 2014;55:1–16.
[22] Murphy MP. How mitochondria produce reactive oxygen species. Biochem J 2009;417(1):1–13.
[23] Paradies G, Paradies V, Ruggiero FM, Petrosillo G. Role of cardiolipin in mitochondrial function and dynamics in Health and disease: molecular and pharmacological aspects. Cells 2019;8(7).
[24] Kulig W, Cwiklik L, Jurkiewicz P, Rog T, Vattulainen I. Cholesterol oxidation products and their biological importance. Chem Phys Lipids 2016;199:144–60.
[25] Marchette LD, Thompson DA, Kravtsova M, Ngansop TN, Mandal MN, Kasus-Jacobi A. Retinol dehydrogenase 12 detoxifies 4-hydroxynonenal in photoreceptor cells. Free Radic Biol Med 2010;48(1):16–25.
[26] Circu ML, Aw TY. Reactive oxygen species, cellular redox systems, and apoptosis. Free Radic Biol Med 2010;48(6):749–62.
[27] Zhuang A, Yang C, Liu Y, Tan Y, Bond ST, Walker S, et al. SOD2 in skeletal muscle: new insights from an inducible deletion model. Redox Biol 2021;47:102135.
[28] Doll S, Proneth B, Tyurina YY, Panzilius E, Kobayashi S, Ingold I, et al. ACSL4 dictates ferroptosis sensitivity by shaping cellular lipid composition. Nat Chem Biol 2017;13(1):91–8.
[29] Yurkova IL, Stuckert F, Kisel MA, Shadyro OI, Arnhold J, Huster D. Formation of phosphatidic acid in stressed mitochondria. Arch Biochem Biophys 2008;480(1):17–26.
[30] Kameoka S, Adachi Y, Okamoto K, Iijima M, Sesaki H. Phosphatidic acid and cardiolipin coordinate mitochondrial dynamics. Trends Cell Biol 2018;28(1):67–76.
[31] Sedlák E, Robinson NC. Phospholipase A2 digestion of cardiolipin bound to bovine cytochrome c oxidase alters both activity and quaternary structure†. Biochemistry 1999;38(45):14966–72.
[32] Musatov A, Robinson NC. Bound cardiolipin is essential for cytochrome c oxidase proton translocation. Biochimie 2014;105:159–64.
[33] Wu L, Chaudhary SC, Atigadda VR, Belyaeva OV, Harville SR, Elmets CA, et al. Retinoid X receptor agonists upregulate genes responsible for the biosynthesis of all-trans-retinoic acid in human epidermis. PLoS One 2016;11(4):e0153556. -e.
[34] Belyaeva OV, Wu L, Shmarakov I, Nelson PS, Kedishvili NY. Retinol dehydrogenase 11 is essential for the maintenance of retinol homeostasis in liver and testis in mice. J Biol Chem 2018;293(18):6996–7007.
[35] Rolfs Z, Frey BL, Shi X, Kawai Y, Smith LM, Welham NV. An atlas of protein turnover rates in mouse tissues. Nat Commun 2021;12(1):6778.
[36] Horton JD, Bashmakov Y, Shimomura I, Shimano H. Regulation of sterol regulatory element binding proteins in livers of fasted and refed mice. Proc Natl Acad Sci USA 1998;95(11):5987–92.
[37] Ge SX, Jung D, Yao R. ShinyGO: a graphical gene-set enrichment tool for animals and plants. Bioinformatics 2019;36(8):2628–9.
[38] Kanehisa M, Furumichi M, Sato Y, Ishiguro-Watanabe M, Tanabe M. KEGG: integrating viruses and cellular organisms. Nucleic Acids Res 2020;49(D1):D545–51.
[39] Luo W, Brouwer C. Pathview: an R/Bioconductor package for pathway-based data integration and visualization. Bioinformatics 2013;29(14):1830–1.
[40] Hartley JL, Temple GF, Brasch MA. DNA cloning using in vitro site-specific recombination. Genome Res 2000;10(11):1788–95.
[41] Livak KJ, Schmittgen TD. Analysis of relative gene expression data using real-time quantitative PCR and the 2(-Delta Delta C(T)) Method. Methods 2001;25(4):402–8.
[42] Weir JM, Wong G, Barlow CK, Greeve MA, Kowalczyk A, Almasy L, et al. Plasma lipid profiling in a large population-based cohort. J Lipid Res 2013;54(10):2898–908.
[43] Huynh K, Barlow CK, Jayawardana KS, Weir JM, Mellett NA, Cinel M, et al. High-throughput plasma lipidomics: detailed mapping of the associations with cardiometabolic risk factors. Cell Chem Biol 2019;26(1):71–84.e4.
[44] Bond ST, King EJ, Henstridge DC, Tran A, Moody SC, Yang C, et al. Deletion of Trim28 in committed adipocytes promotes obesity but preserves glucose tolerance. Nat Commun 2021;12(1):74.

